

OPEN ACCESS

The effect of BZO dopant concentration on magnetically obtained B_{irr} and B_{c2} in YBCO thin films deposited on STO substrates

To cite this article: P Paturi *et al* 2014 *J. Phys.: Conf. Ser.* **507** 012040

View the [article online](#) for updates and enhancements.

You may also like

- [Controllable subwavelength-ripple and -dot structures on \$YBa_2Cu_3O_7\$ induced by ultrashort laser pulses](#)
C W Luo, W T Tang, H I Wang *et al.*
- [Electron mass anisotropy of \$BaZrO_3\$ doped YBCO thin films in pulsed magnetic fields up to 30 T](#)
H Palonen, H Huhtinen, M A Shakhov *et al.*
- [Effect of surface modification of \$CeO_2\$ buffer layers on \$J_c\$ and defect microstructures of large-area YBCO thin films](#)
K Develos-Bagarinao, H Yamasaki and Y Nakagawa



ECS
The
Electrochemical
Society
Advancing solid state &
electrochemical science & technology

DISCOVER
how sustainability
intersects with
electrochemistry & solid
state science research

The effect of BZO dopant concentration on magnetically obtained B_{irr} and B_{c2} in YBCO thin films deposited on STO substrates

P Paturi¹, M Malmivirta¹, H Palonen^{1,2} and H Huhtinen¹

¹ Wihuri Physical Laboratory, Department of Physics and Astronomy, University of Turku, 20014 Turku, Finland

² National Graduate School on Nanoscience, Finland

E-mail: petriina.paturi@utu.fi

Abstract. The effect of BaZrO₃ (BZO) dopant concentration (0-9 wt-%) on magnetically obtained irreversibility field B_{irr} and upper critical field B_{c2} is investigated in YBa₂Cu₃O_{6+x} (YBCO) thin films prepared by pulsed laser deposition on SrTiO₃ (001) (STO) substrates. It is found that the magnetic determination of B_{irr} and B_{c2} works well. The results show that BZO-doping increases B_{c2} in all concentrations, implying a change in the coherence length and band structure of the superconductor.

1. Introduction

In preparation of superconducting wires for applications, the flux pinning properties of the superconductor are essential. For most applications, isotropic dependence of critical current density, J_c , on magnetic field angle is desired and the most common way of inducing it, is by addition of non-superconducting nanorods or -particles. In the past years there has been discussion on how the apparently lowered anisotropy should be interpreted: can the Blatter anisotropy scaling [1], which comes from electron mass anisotropy, be used for analysis of $J_c(\theta)$ curves? Most researchers have recently come to the conclusion that the lowered anisotropy of $J_c(\theta)$ curves is due to strong flux pinning by the nanoinclusions, not a change in electron mass anisotropy. The correct way of measuring the electron mass anisotropy, γ , is from high pulsed magnetic field measurements of resistivity and determination of upper critical field, B_{c2} . Such measurements have been recently published with inconsistent results: in BaZrO₃-doped (BZO) films with nanorods the anisotropy was seen to lower from 5 of undoped film to 3.4 in 4% BZO-films [2], but in films with BZO-nanoparticles no lowering of anisotropy was seen [3].

In this paper we test the method presented in [4] to determine the irreversibility field, B_{irr} and B_{c2} . These are determined for YBa₂Cu₃O_{6+x} films doped with varying amounts of BZO. We compare the results to those made in high fields for similar samples [2] and also resistive measurements at low fields from the same films [5].

2. Experimental

The YBCO thin films were deposited by pulsed laser ablation from five differently BZO-doped nanograined targets on single crystal SrTiO₃ (100) (STO) substrates. The targets were prepared



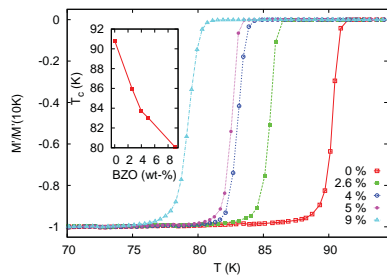


Figure 1. The normalized real parts of the ac-magnetization for all the films. The inset shows the dependence of T_c on temperature.

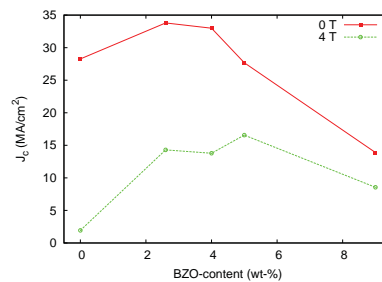


Figure 2. J_c of all the films in 0 T and 4 T determined from hysteresis loops measured at 10 K.

using the citrate-gel method [6] adding the BZO already in the sol-phase. The BZO contents of the targets were 0, 2.6, 4, 5 and 9 wt-%. The used ablation parameters were optimized for J_c and the substrate temperature was 770 °C and the ablation pressure was 23 Pa. The detailed deposition conditions can be found at [2]. At this substrate temperature the BZO forms straight 5-7 nm diameter rods perpendicular to the surface of the substrate [7].

The critical temperatures, T_c , of the films were determined using the ac-magnetometry option in a Quantum Design PPMS with zero dc-field and 0.1 mT ac-field at 113 Hz frequency. The real parts of the magnetizations are shown in Fig. 1. T_c was defined as the temperature where the reduced magnetization is -0.1. The transition widths, ΔT_c were defined as the temperature difference between -0.9 and -0.1 values of the reduced magnetization. For all the samples ΔT_c was between 1.3 and 2 K with no clear dependence on BZO-content. The films show typical decrease of T_c with increasing BZO-content [8], but as the transition widths show, the quality of all the films is good.

The critical current densities, J_c , were determined from magnetization loops measured at 10 K between -8 and 8 T using the Bean critical state model [9]. The obtained critical current densities in zero field and in 4 T are shown in Fig. 2. It can be seen that at zero field the 2.6 % and the 4 % sample give the highest J_c , but at 4 T the highest J_c is obtained with the 5 % sample. This is in accordance with our previous results [10] where it was found that the optimal BZO-content increases with increasing magnetic field. The obtained values of J_c show that the samples are highly optimized also for critical current density.

The upper critical field, B_{c2} , and the irreversibility field, B_{irr} , were determined using the method introduced in [4]. Using the PPMS dc-magnetization option the zero field cooled, ZFC, and field cooled, FC, temperature dependent magnetizations were measured at fields of 0, 0.125, 0.25, 0.5, 1, 2, 4, 6 and 8 T. The irreversibility temperature for the measurement magnetic field, T_{irr} , was determined as the temperature where the ZFC and FC curves deviate from each other (Fig. 3). Similarly, the critical temperature related to the upper critical field, T_{c2} , was defined as the temperature where both the ZFC and FC curves deviate from the constant diamagnetic signal given by the STO substrate. The obtained temperatures define the temperature dependences of B_{c2} and B_{irr} .

3. Results and discussion

The overall shape of the ZFC and FC curves can be explained using the critical state models and vortex compression models [11, 12, 13]. In ZFC the sample is cooled down in zero field and then at low temperature the measurement field is switched on. The vortices penetrate the superconductor according to the critical state model and a large diamagnetic signal is observed

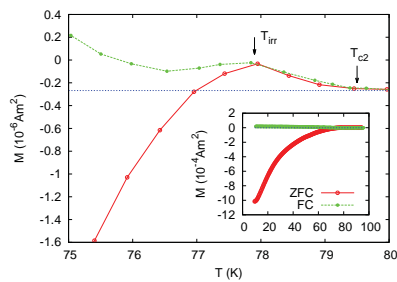


Figure 3. The definition of T_{irr} and T_{c2} for the 5 wt-% BZO sample in magnetic field of 1 T. The temperature independent diamagnetic signal given by the STO substrate shown as a blue line. The inset shows the full ZFC and FC curves.

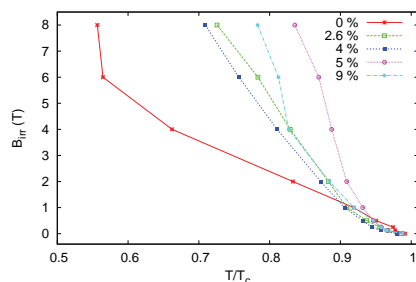


Figure 4. The temperature dependence of B_{irr} for all the samples.

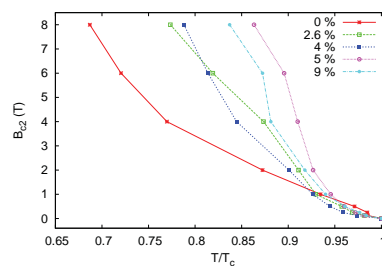


Figure 5. The temperature dependence of B_{c2} for all the samples.

(inset of Fig. 3). As the temperature is increased, the vortices move more into the sample and the diamagnetic signal decreases. Close to the critical temperature, a paramagnetic signal is observed. The origin of this paramagnetic signal has been discussed earlier [11, 12, 13], and in general it is thought to arise from the compression of the vortices away from the surface by the shielding currents. In all of our measurements the ZFC curve has a maximum at T_{irr} , *i.e.* where the vortices are not pinned anymore. It is natural that the highest compression and paramagnetic signal is obtained just before the vortices are free to move. Above T_{irr} the magnetization approaches zero, which it reaches at T_c . The maximum in the ZFC is observed in all our measurements regardless of external field, but the shape of the ZFC curve has been observed to depend on both the external field and the length of the measurement scan [12].

During field cooling the field fully penetrates the sample above T_c and upon cooling the vortices are formed and compressed to show a paramagnetic response. At T_{irr} the ZFC and FC curves deviate and the FC curve continues to give a paramagnetic signal. Below T_{irr} the signal slightly increases due to further compression of the vortices, which is caused mainly by the increase of J_c with temperature [12].

The determined irreversibility fields for all the samples are shown in Fig. 4. The $B_{\text{irr}}(T)$ of all the doped films are fairly close to each other, but the undoped film is clearly different from these. At low temperatures the undoped film has lowest B_{irr} and the 5% doped sample has highest. Around $T = 0.94 T_c$ there is a crossover above which the undoped sample has the highest B_{irr} . The result at low temperature is easily understood to be caused by the strong pinning by the BZO-rods. The rods form much stronger pinning sites for the vortices than the dislocations prevalent in the undoped sample, which increases B_{irr} . Close to the critical temperature the undoped sample is better probably due to more homogeneous material.

The determined upper critical fields show (Fig. 5) a similar tendency as the B_{irr} . B_{c2} of the doped films are clearly higher than those of the undoped film, although the difference is not as large as in B_{irr} . This is in line with the previous observations for BaHfO₃-doped films [4] as well

as data from pulsed high fields [2]. Increase in B_{c2} implies a decrease in the Ginzburg-Landau coherence length, ξ . According to the BCS-theory the ξ depends on the superconducting gap and the Fermi-velocity, *i.e.* BZO-doping causes a change in the band structure of YBCO. The ξ can also change when the superconductor shifts from the clean limit to dirty limit. This effect is most notable at high temperature, where it can explain the increase of B_{c2} , but at lower temperatures, $T < 0.9 T_c$, the distance between the BZO-rods is much larger than ξ and the decrease of the electron mean free path is not enough to explain the two-fold increase in B_{c2} .

When these data are compared to the resistive data from the same samples [5], we can see that this method of determining the B_{c2} from magnetic measurements is actually closer to the “correct” high field measurements. Both methods give higher B_{c2} for the BZO-doped films, where as the low current and constant field measurements give similar values for all samples except the 9 wt-%, where B_{c2} is lower. This is easily understood as the low current resistive measurements probe only the very best superconducting paths in the samples.

In [2] it was seen that for 4 % -doped YBCO the increase of B_{c2} is connected to lower electron mass anisotropy ($\gamma = 3.4$ for BZO-doped film). Since the BZO-nanorods are only about 20 nm apart, it is plausible that the strain they cause to the YBCO lattice, also would have an effect for the band structure. Naturally, based on data from only one orientation, we cannot say anything about the electron mass anisotropy for these films, but since the results are similar as in [2], it can be assumed that the electron mass anisotropy is lowered also for the other BZO-concentrations.

4. Conclusions

We have magnetically measured thin YBCO films with different BZO-concentrations and determined the B_{irr} and B_{c2} from ZFC and FC measurements. It was found that the method works well, specially for the determination of B_{c2} . It was found that the BZO-doping increases B_{irr} for all the samples as was expected. The B_{c2} was also found to increase for all the BZO-doped films. This implies a change in the band structure of YBCO and is consistent with the results from high magnetic field measurements [2].

5. Acknowledgments

Jenny and Antti Wihuri Foundation is acknowledged for financial support. M. M. acknowledges Finnish Foundation for Technology Promotion and Finnish Cultural Foundation for financial support.

References

- [1] Blatter G, Feigel'man M V, Geshkenbein V B, Larkin A I and Vinokur V M 1994 *Reviews of Modern Physics* **66** 1125
- [2] Palonen H, Huhtinen H, Shakhov M A and Paturi P 2013 *Supercond. Sci. Technol.* **26** 045003
- [3] Llordés A, Palau A, Gázquez J, Coll M, Vlad R, Pomar A, Arbiol J, Guzmán R, Ye S, Rouco V, Sandiumenge F, Ricart S, Puig T, Varela M, Chateigner D, Vanacken J, Gutiérrez J, Moshchalkov V, Deutscher G, Magen C and Obradors X 2012 *Nat. Mater.* **11** 329
- [4] Matsushita T, Nagamizu H, Tanabe K, Kiuchi M, Otabe E S, Tobita H, Yoshizumi M, Izumi T, Shiohara Y, Yokoe D, Kato T and Hirayama T 2012 *Supercond. Sci. Technol.* **25** 125003
- [5] Malmivirta M, Palonen H, Huhtinen H and Paturi P 2013 *Journal of Physics: Conference Series* **submitted**
- [6] Raittila J, Peurla M, Huhtinen H, Paturi P and Laiho R 2003 *Physica C* accepted
- [7] Malmivirta M, Yao L, Huhtinen H, Palonen H, van Dijken S and Paturi P 2013 *J. Appl. Phys.* **submitted**
- [8] Peurla M, Paturi P, Stepanov Y P, Huhtinen H, Tse Y Y, Bódi A C, Raittila J and Laiho R 2006 *Supercond. Sci. Technol.* **19** 767–771
- [9] Wiesinger H P, Sauerzopf F M and Weber H W 1992 *Physica C* **203** 121
- [10] Huhtinen H, Irjala M, Paturi P, Shakhov M A and Laiho R 2010 *J. Appl. Phys.* **107** 053906
- [11] Koshelev A E and Larkin A I 1995 *Phys. Rev. B* **52** 13559
- [12] Luzhbin D A, Pan A V, Komashko V A, Flis V S, Pan V M, Dou S X and Esquinazi P 2004 *Phys. Rev. B* **69** 024506
- [13] Moshchalkov V V, Qiu X G and Bruyndoncx V 1997 *Phys. Rev. B* **55** 11793